NANO · MICRO small
www.small-journal.com

# Light-Driven Reversible Hydrogen Storage in Light-Weight Metal Hydrides Enabled by Photothermal Effect

*Yahui Sun, Xiaoyue Zhang, Wei Chen, Jikai Ye, Shunlong Ju, Kondo-Francois Aguey-Zinsou, Guanglin Xia,* Dalin Sun, and Xuebin Yu**

**Requiring high temperature for hydrogen storage is the main feature impeding practical application of light metal hydrides. Herein, to lift the restrictions associated with traditional electric heating, light is used as an alternative energy input, and a light-mediated catalytic strategy coupling photothermal and catalytic effects is proposed. With $NaAlH_4$ as the initial target material, $TiO_2$ nanoparticles uniformly distribute on carbon nanosheets ($TiO_2$@C), which couples the catalytic effect of $TiO_2$ and photothermal property of C, is constructed to drive reversible hydrogen storage in $NaAlH_4$ under light irradiation. Under the catalysis of $TiO_2$@C, complete hydrogen release from $NaAlH_4$ is achieved within 7 min under a light intensity of 10 sun. Furthermore, owing to the stable catalytic and photothermal effect of $TiO_2$@C, $NaAlH_4$ delivers a reversible capacity of 4 wt% after 10 cycles with a capacity retention of 85% under light irradiation only. The proposed strategy is also applicable to other light metal hydrides such as $LiAlH_4$ and $MgH_2$, validating its universality. The concept of light-driven hydrogen storage provides an alternative approach to electric heating, and the light-mediated catalytic strategy proposed herein paves the way to the design of reversible high-density hydrogen storage systems that do not rely on artificial energy.**

## 1. Introduction

Hydrogen energy, as the cleanest renewable resource and the primary alternative to traditional fossil energy, is of vital significance in addressing the ever-increasing global energy shortage and environmental pollution issues. The lack of efficient techniques for the safe and compact storage of hydrogen, however, remains a major bottleneck for realizing the hydrogen energy future. Owing to their stability under ambient conditions and high gravimetric and volumetric hydrogen densities, light-weight metal hydrides have received ever-growing attention as potential hydrogen storage materials. The high operating temperature of these metal hydrides induced by high thermodynamic stability and kinetic barrier, however, poses a critical challenge for their practical application.[1] For instance, as a representative metal hydride, $NaAlH_4$ with a gravimetric and volumetric hydrogen density of 7.5 wt% and 94 g $L^{-1}$, respectively, is the only known light-weight metal hydrides that holds favorable enthalpies of 37 and 47 kJ $mol^{-1}$ $H_2$ for two-step reversible hydrogen storage, corresponding to a theoretical operating temperature of ≈100 °C under 1 atm $H_2$.[2] However, the high kinetic barriers, owing to the sluggish diffusion of hydrogen and mass transport, results in a significantly higher operating temperature for practical hydrogen storage. Although the hydrogen storage performance of $NaAlH_4$ has been remarkably improved via various strategies, including catalysis,[3] nanosizing,[4] and thermodynamic destabilization,[5] the operating temperature for its reversible hydrogen storage is still as high as 150 °C. Moreover, for other light-weight metal hydrides that are generally with higher thermodynamic stability than $NaAlH_4$, even higher operating temperatures are required.[6] As a result, in laboratory and in practice, electric heaters are inevitably required to thermally drive the reversible $H_2$ uptake/release processes of these metal hydrides, which not only consumes artificial energy (i.e., electricity), but also adds on to the weight of the integrated system, significantly lowering the hydrogen density and energy efficiency of the whole hydrogen storage system.

Solar energy, a non-polluting, renewable and economical energy source, has been widely regarded and developed as an ideal substitute for present reliance on electrically induced heat.[7] Inspired by this progress, we propose a light-mediated catalytic strategy to realize reversible hydrogen storage in metal hydrides using solar as the only energy source by coupling catalytic and photothermal effects (**Figure 1**a). The hypothesis is that the temperature required for hydrogen uptake/release would be lowered with effective catalysis, while an efficient photothermal effect will elevate the temperature of hydrogen storage materials under light. If these two temperatures could match, reversible hydrogen storage should occur with solar as

Y. Sun, X. Zhang, W. Chen, J. Ye, S. Ju, G. Xia, D. Sun, X. Yu
Department of Materials Science
Fudan University
Shanghai 200433, P. R. China
E-mail: xiaguanglin@fudan.edu.cn; yuxuebin@fudan.edu.cn
K.-F. Aguey-Zinsou
Merlin Group
School of Chemistry
The University of Sydney
Sydney, NSW 2006, Australia
The ORCID identification number(s) for the author(s) of this article can be found under https://doi.org/10.1002/smll.202202978.

**DOI: 10.1002/smll.202202978**

 

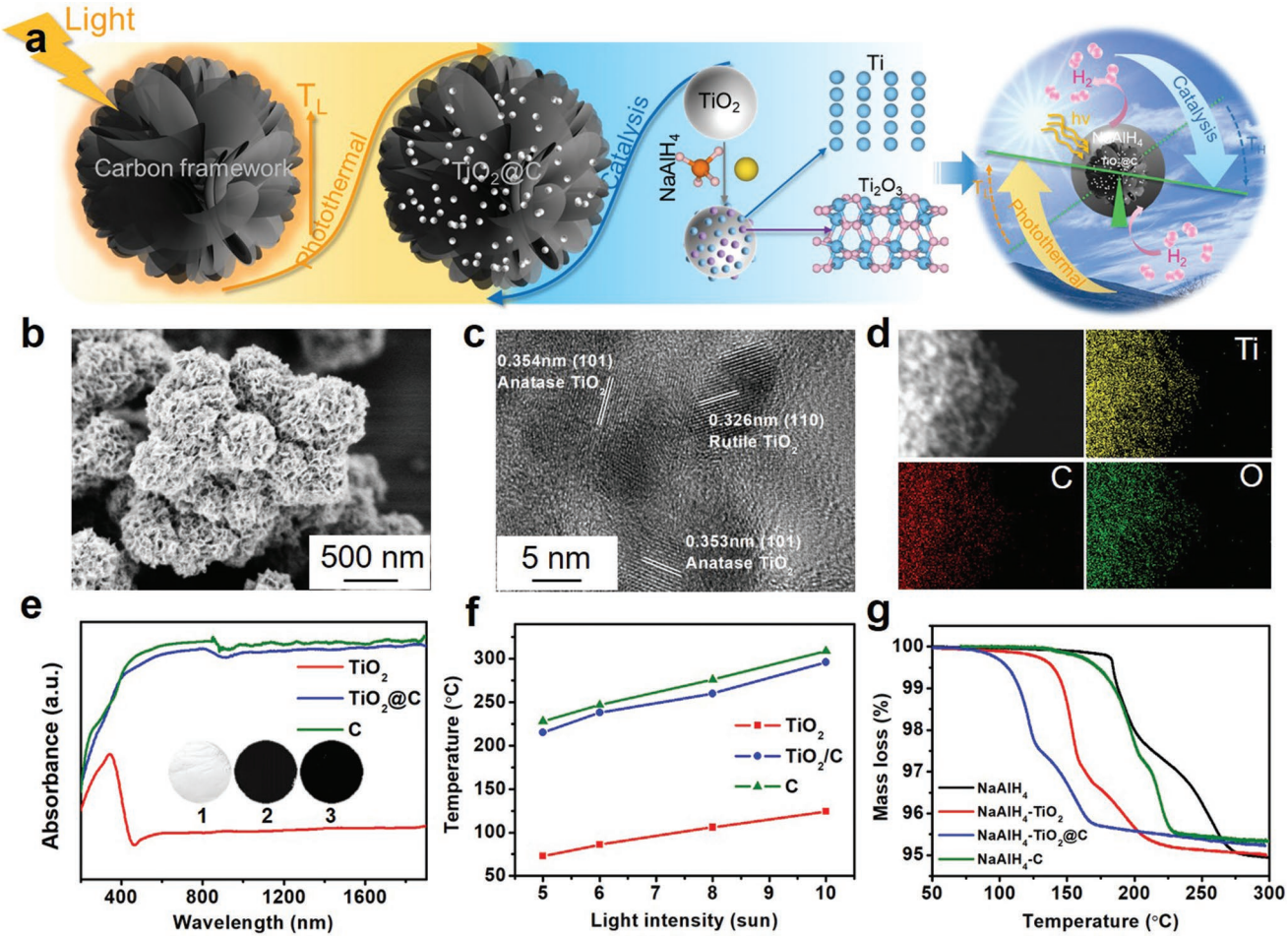


**Figure 1.** a) Schematic diagram of the proposed light-mediated catalytic strategy. b) SEM, c) HRTEM (lattice parameters measured using Gatan Microscopy Suite Software), and d) elemental mapping of $TiO_2$@C. e) UV–vis–NIR spectra of $TiO_2$, $TiO_2$@C, and C (inset: digital photos of 1–$TiO_2$, 2–$TiO_2$@C, and 3–C). f) Photothermal temperatures of $TiO_2$, $TiO_2$@C, and C under various light intensities. g) TPD profiles of $NaAlH_4$, $NaAlH_4$-$TiO_2$, $NaAlH_4$-$TiO_2$@C, and $NaAlH_4$-C.

the only energy input. The key to implementing this proposed strategy is to design catalysts with desired catalytic and photothermal properties, which could not only effectively lower the operating temperature for hydrogen uptake/release but also play a photothermal role in increasing the temperature of metal hydrides using light.

To validate the proposed strategy and concept, in this study, $NaAlH_4$ is taken as the initial target hydrogen storage material and a $TiO_2$@C (i.e., $TiO_2$ nanoparticles uniformly distributed on a carbon framework) catalyst is constructed to integrate the catalytic effect of $TiO_2$[8] and the photothermal effect of C.[9] $TiO_2$ and C are selected as the functional components owing to their easy accessibility and high efficiency. The efficient photothermal effect of C is expected to rapidly elevate the temperature of $NaAlH_4$ upon light irradiation while the catalytic role of $TiO_2$ lowering the temperatures required for hydrogen storage reactions, realizing light-driven reversible hydrogen storage (Figure 1a). As a result, under the catalysis of $TiO_2$@C, $NaAlH_4$ fully released hydrogen within 7 min under a light intensity of 10 sun. Furthermore, owing to the superior catalytic and photothermal effect of $TiO_2$@C, reversible hydrogen storage in $NaAlH_4$ with a capacity of ≈4 wt% is successfully achieved using full-spectrum light irradiation only. Moreover, the strategy is verified to be universal and can be applied to other light-weight metal hydrides, such as $LiAlH_4$ and $MgH_2$. This study validates the concept of light-driven reversible hydrogen storage, opening a new direction for the design and development of reversible high-density hydrogen storage systems for mobile applications.

## 2. Results and Discussion

### 2.1. Preparation and the Photothermal Effect of $TiO_2$@C

The morphology of as-synthesized $TiO_2$@C was revealed to be flowerlike with an average size of around 500 nm (Figure 1b) constructed by carbon nanosheets, in which anatase $TiO_2$ and rutile $TiO_2$ nanoparticles (Figure S2a, Supporting Information) of around 10 nm are uniformly distributed (Figure 1c). Besides $Ti^{4+}$, which is the dominant Ti species, X-ray photoelectron spectroscopy (XPS) measurement (Figure S2c, Supporting Information) demonstrates the presence of slight amount of

$Ti^{3+}$. Moreover, C–O–C and C–O–Ti interactions were identified from the O 1s and C 1s XPS spectra (Figure S2d,e, Supporting Information), confirming the stable anchoring of $TiO_2$ nanoparticles on the carbon nanosheets, which could prevent the agglomeration of $TiO_2$ nanoparticles toward well-preserved catalytic effect. As revealed by elemental mapping (Figure 1d), the elements of Ti, O, and C are well overlapped, indicating the uniform dispersion of $TiO_2$ nanoparticles inside of the carbon framework. Thermogravimetric analysis (TGA) measurement of the as-synthesized $TiO_2$@C (Figure S2b, Supporting Information) suggests that C accounts for around 36.7% of the total mass of $TiO_2$@C.

Owing to its high content of carbon with broadband light absorption, the as-synthesized $TiO_2$@C displays efficient light absorbance across the full spectrum, which is only slightly lower than pure C (Figure 1e). By comparison, $TiO_2$ only absorbs light in the UV range with considerably lower absorbance (Figure 1e). The light absorbance difference of the materials could be macroscopically reflected by their colors (inset of Figure 1e). $TiO_2$ has a white color while $TiO_2$@C appears to be black, and C is even slightly darker than $TiO_2$@C. Correspondingly, $TiO_2$@C and C exhibit significantly superior photothermal performance compared to $TiO_2$, resulting in photothermal temperatures that are over 150 °C higher than that of $TiO_2$ under each light intensity (Figure 1f). Particularly, under a light intensity of 10 sun, an equilibrium photothermal temperature as high as 296 and 310 °C could be achieved for $TiO_2$@C and C, respectively. In sharp contrast, the temperature of $TiO_2$ was only 124 °C under the identical condition. In addition, the equilibrium temperature turns out to be in a near-linear relationship with the light intensity for each material, but the temperature elevation along with light intensity increase is more significant for $TiO_2$@C and C. Increasing the light intensity from 5 to 10 sun, the equilibrium temperature of $TiO_2$@C and C could be elevated from 215 to 296 °C and from 228 to 309 °C, respectively, presenting a temperature elevation of 81 and 82 °C correspondingly. By comparison, the increase of equilibrium temperature is limited to be only 51 °C for $TiO_2$. This phenomenon validates that, owing to the uniform distribution of carbon frameworks with robust interaction with $TiO_2$, $TiO_2$@C exhibits superior photothermal conversion ability with rapid response to light, which is much superior than that of $TiO_2$ and even comparable with pure C (Figure S3, Supporting Information).

### 2.2. Catalytic Effect of $TiO_2$@C

After the introduction of C via facile mechanical milling process, the characteristic XRD peaks of $NaAlH_4$ could be well preserved (Figure S4, Supporting Information). Interestingly, the introduction of $TiO_2$@C or $TiO_2$ resulted in partial dehydrogenation of $NaAlH_4$ into $Na_3AlH_6$ and Al during the milling process and a more significant dehydrogenation degree could be observed for $NaAlH_4$-$TiO_2$@C in comparison. This phenomenon indicates the catalytic capability of $TiO_2$@C in promoting hydrogen desorption from $NaAlH_4$ even during the milling process.[10] Ti 2p XPS spectra of as-milled $NaAlH_4$-$TiO_2$ and $NaAlH_4$-$TiO_2$@C verifies the reduction of $TiO_2$ after the milling process with the formation of metallic Ti and $Ti_2O_3$ (Figure S5, Supporting Information), which have been experimentally regarded as effective catalysts to enhance hydrogen desorption performance of $NaAlH_4$.[8a] Theoretical calculations by using density functional theory (DFT) reveal that four Al—H bonds of the pristine $NaAlH_4$ monomer have an equal length of 1.641 Å. Upon interacting with Ti and $Ti_2O_3$, the corresponding Al—H bonds of $NaAlH_4$ are stretched with an average increase of bond length to1.677 and 1.655 Å, respectively, which demonstrates that Ti and $Ti_2O_3$ are capable of weakening Al—H bonds effectively and hence pose a catalytic effect on $NaAlH_4$.

The capability of $TiO_2$@C in catalytically improving hydrogen storage performance of $NaAlH_4$ is experimentally investigated using temperature-programmed desorption (TPD) method. As shown in Figure 1g, the ball-milled $NaAlH_4$ without any additives has a temperature window of 180–275 °C for hydrogen desorption. Although C exhibits superior photothermal performance than both $TiO_2$ and $TiO_2$@C, only limited catalytic effect in improving hydrogen storage property of $NaAlH_4$ could be observed. By comparison, the onset temperature for hydrogen desorption from $NaAlH_4$ under the catalysis of $TiO_2$ could be effectively reduced to ≈125 °C with most hydrogen released before 210 °C, which directly demonstrates the catalytic role of $TiO_2$ in enhancing hydrogen storage performance of $NaAlH_4$. Interestingly, under the catalysis of $TiO_2$@C, an onset temperature as low as 90 °C could be observed for $NaAlH_4$, accompanied with complete dehydrogenation before 170 °C, 40 °C lower than that of $NaAlH_4$ catalyzed by $TiO_2$. This result provides direct evidence to the superior catalytic effect of $TiO_2$@C than $TiO_2$ owing to the decrease of particle size of $TiO_2$ down to nanometer scale, which could effectively promote the physical contact between $TiO_2$ and $NaAlH_4$ and hence the catalytic role of $TiO_2$ in improving hydrogen desorption performance of $NaAlH_4$.

### 2.3. Light-Driven Hydrogen Storage Performance of $NaAlH_4$

Based on the above-mentioned results, it is concluded that $TiO_2$@C designed and synthesized herein successfully integrates the photothermal effect of C and the catalytic effect of $TiO_2$, which is expected to elevate the photothermal temperature while lowering hydrogen storage reaction temperature of $NaAlH_4$ toward light-driven hydrogen storage of $NaAlH_4$ (Figure 1a). UV–vis–NIR measurement (**Figure 2**a) demonstrates that only limited light absorbance could be observed for ball-milled $NaAlH_4$. It is interesting to note that, despite the limited light absorbance of $TiO_2$ (Figure 1e), the light absorbance of $NaAlH_4$ ball-milled with $TiO_2$ is increased to a relatively high level, which could be attributed to the formation of surface $Ti^0$ and $Ti^{3+}$ species with broader light absorbance than $TiO_2$[11] induced by the partial reduction of $TiO_2$ during the milling process (Figure S5, Supporting Information). By comparison, owing to the efficient light absorbance of $TiO_2$@C and C (Figure 1e), the as-prepared $NaAlH_4$-$TiO_2$@C and $NaAlH_4$-C display significantly higher light absorbance than that of $NaAlH_4$-$TiO_2$ (Figure 2a). As a result, under a light intensity of 10 sun (1 sun = 100 mw $cm^{-2}$), the equilibrium photothermal temperatures of the materials are verified to be following the same sequence of their light absorbance properties, being

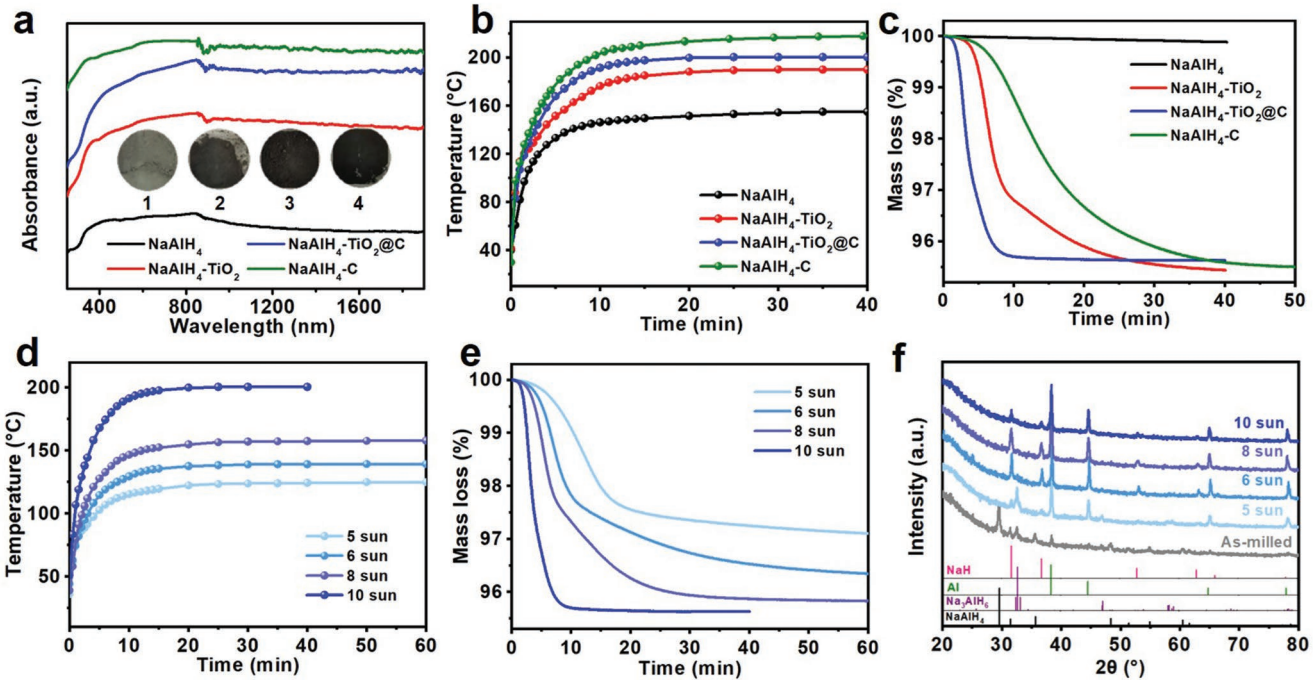


**Figure 2.** a) UV–vis–NIR spectra of $NaAlH_4$, $NaAlH_4$-$TiO_2$, $NaAlH_4$-$TiO_2$@C, and $NaAlH_4$-C (inset: digital photos of 1–$NaAlH_4$, 2–$NaAlH_4$-$TiO_2$, 3–$NaAlH_4$-$TiO_2$@C, and 4–$NaAlH_4$-C). b) Photothermal temperature profiles and c) hydrogen desorption profiles $NaAlH_4$, $NaAlH_4$-$TiO_2$, $NaAlH_4$-$TiO_2$@C, and $NaAlH_4$-C under a light irradiation intensity of 10 sun. d) Temperature profiles and e) hydrogen release profiles of $NaAlH_4$-$TiO_2$@C under various light intensities. f) XRD patterns of the light-driven dehydrogenation products of $NaAlH_4$-$TiO_2$@C under various light intensities.

219 °C for $NaAlH_4$-C, 202 °C for $NaAlH_4$-$TiO_2$@C, and 189 °C for $NaAlH_4$-$TiO_2$, respectively. In sharp contrast, only a temperature of 154 °C could be obtained for pure $NaAlH_4$ (Figure 2b). Owing to the coupled effect of the superior photothermal performance and catalytic effect of $TiO_2$@C, the photothermal temperature (202 °C) of $NaAlH_4$-$TiO_2$@C is sufficient for its complete hydrogen desorption, which could be achieved before 170 °C under direct thermal heating (Figure 1g). Accordingly, complete hydrogen desorption is rapidly achieved for $NaAlH_4$-$TiO_2$@C within 7 min only under 10 sun light irradiation (Figure 2c and Figure S4b, Supporting Information). By comparison, no hydrogen desorption could be observed for $NaAlH_4$ under the identical condition, which could be attributed to the mismatch between the temperature achieved under light irradiation (154 °C) and that required for its hydrogen desorption (>180 °C) (Figures 2b and 1g). Interestingly, even with the limited catalytic effect of C, $NaAlH_4$-C is still capable of releasing its hydrogen completely, which demonstrates the capability of C with high photothermal conversion efficiency in elevating the temperature of $NaAlH_4$ toward hydrogen desorption. The time required for complete dehydrogenation, however, reaches 40 min for $NaAlH_4$-C, almost 7 times longer than that of $NaAlH_4$-$TiO_2$@C, validating that the superior catalytic role of $TiO_2$@C than that of C plays an additional role in enhancing light-driven hydrogen desorption performance of $NaAlH_4$. On the other hand, although the photothermal property of $TiO_2$ is much lower than that of C, only a time of 25 min is required for complete dehydrogenation of $NaAlH_4$-$TiO_2$, which demonstrates that the match of the decreased hydrogen desorption temperature induced by catalytic role of $TiO_2$ with the equilibrium temperature that is achieved by the photothermal effect of $NaAlH_4$-$TiO_2$ is also able to realize complete hydrogen desorption (Figure 2c). These results directly verify our proposed strategy in realizing fast light-driven hydrogen desorption via coupling catalytic and photothermal effects of $TiO_2$@C, which could decrease hydrogen desorption temperature of $NaAlH_4$ and simultaneously elevate the equilibrium temperature under light irradiation. Meanwhile, comparing the experimental results of the $NaAlH_4$ materials, a higher matching degree between the two temperatures would result in a faster hydrogen desorption process. The $NaAlH_4$ materials go through phase change from $NaAlH_4$ to NaH and Al during the dehydrogenation process. In order to verify whether this phase change influences the light absorbance and photothermal effect of the materials, UV–vis–NIR spectra of the light-driven dehydrogenation products of $NaAlH_4$-$TiO_2$, $NaAlH_4$-$TiO_2$@C, and $NaAlH_4$-C were measured (Figure S4c, Supporting Information). Meanwhile, pure $NaAlH_4$ was fully dehydrogenated under electric heating, and the dehydrogenation product was also subjected to UV–vis–NIR measurement to provide reference. For pure $NaAlH_4$, the intensity of the UV–vis–NIR spectrum enhanced considerably after hydrogen desorption, indicating a better light absorbance of the dehydrogenation products than that of $NaAlH_4$. However, under the influence of catalysts, which remarkably enhanced the light absorbance of the starting $NaAlH_4$ materials, the effect of this phase change on light absorbance is not as significant. Specifically, for $NaAlH_4$-$TiO_2$, the light absorbance enhanced to some extent after hydrogen

desorption but not as significant as that for $NaAlH_4$, while the light absorbance basically remained stable at an outstandingly high level for $NaAlH_4$-$TiO_2$@C and $NaAlH_4$-C despite the phase change from $NaAlH_4$ to NaH and Al. The results indicate that in the presence of components with significantly superior light absorbance (e.g., $TiO_2$@C and C) as the main light absorber, the light absorbance and photothermal effect of the material can remain stable regardless of the phase state of $NaAlH_4$.

Subsequently, light-driven hydrogen desorption properties of $NaAlH_4$-$TiO_2$@C were evaluated under various light intensities (Figure 2d,e), which indicates that a higher light intensity results in a higher photothermal temperature, and thus a faster and more complete hydrogen desorption process (Figure 2f). Specifically, the equilibrium temperature of $NaAlH_4$-$TiO_2$@C reaches 125, 140, 158, and 202 °C under 5, 6, 8, and 10 sun, respectively (Figure 2a). As indicated by the corresponding light-driven hydrogen desorption profiles (Figure 2e), the equilibrium temperature of $NaAlH_4$-$TiO_2$@C (158 °C) under 8 sun is still sufficient for complete hydrogen desorption. Even under a low light intensity of 5 sun, $NaAlH_4$ under the catalysis of $TiO_2$@C manages to release ≈2.5 wt% $H_2$ within 30 min (Figure 2e), corresponding to the completion of the first dehydrogenation step from $NaAlH_4$ to $Na_3AlH_6$ and Al and a small extent of the decomposition of $Na_3AlH_6$ (Figure 2f).

In addition, the comparison between light irradiation and traditional electric heating in driving hydrogen desorption performance of $NaAlH_4$-$TiO_2$@C is investigated in detail. When the temperature profiles obtained by electric heating has a high matching degree with that under each light intensity, comparable hydrogen desorption behaviors could be observed for $NaAlH_4$-$TiO_2$@C driven by light irradiation and electric heating (Figure S7, Supporting Information). Slight difference could be observed; however, it is considered to be insignificant and is likely to be caused by temperature control and measurement errors. To further validate our initial observation on the equivalent effect of light irradiation to electric heating, the apparent activation energy ($E_a$) of $NaAlH_4$ under the catalysis of $TiO_2$@C was calculated based on its corresponding hydrogen desorption profiles (Figure S7b,d,f,h, Supporting Information) according to the Arrhenius equation (Figure S8, Supporting Information).[12] The $E_a$ is determined to be 55.7 ± 1.4 kJ $mol^{-1}$ $H_2$ for $NaAlH_4$-$TiO_2$@C under light irradiation, comparable to that under electric heating (58.2 ± 1.9 kJ $mol^{-1}$ $H_2$). This result further demonstrates that light irradiation is a feasible alternative energy input for hydrogen storage in $NaAlH_4$. More importantly, in comparison to hydrogen desorption driven by traditional electric heating, light-driven hydrogen desorption has an advantage of fast response to energy input. As presented in **Figure 3**a,b, when an electric heater pre-heated to 200 °C was used to provide energy, it took 6 min before $NaAlH_4$-$TiO_2$@C was heated to a temperature sufficient to trigger the hydrogen release process; and upon removing the electric heater, $NaAlH_4$-$TiO_2$@C kept releasing hydrogen for around 3 min before cooled down. This lag of response could be clearly observed for initial three cycles due to slow heat conduction. By comparison, when replacing the electric heater with light, $NaAlH_4$-$TiO_2$@C is able to release hydrogen almost immediately upon turning on the light, and stop releasing hydrogen within 10 s when the light was off. The response time is only around 5% of that when applying an electric heater, which could be further demonstrated by initial three light on/off cycles. The rapid response of the hydrogen release process to light is induced by the fast response feature of photothermal effect, i.e., the material temperature responses rapidly to light irradiation and thereby the hydrogen release process can be well controlled by adjusting the light.

In order to verify if our proposed strategy is also feasible for the hydrogen uptake process to achieve light-driven reversible hydrogen storage, the cycling performance of $NaAlH_4$-$TiO_2$@C is evaluated under light irradiation (Figure S9, Supporting Information). Specifically, light-driven hydrogen desorption is carried out under static vacuum with a light intensity of 10 sun; and since hydrogen absorption normally requires lower temperature, a light intensity of 5 sun was applied for reversible hydrogen uptake under a static hydrogen pressure of 8 MPa. Hydrogen uptake process could be directly reflected by the pressure change curve recorded (Figure 3d), which indicates that the hydrogen absorption can be completed within 1 h under the current experimental conditions as featured by the stabilization of pressure. Therefore, the hydrogen uptake time for each cycle of the cycling test was kept for 1 h and the hydrogen uptake content could be determined by the following hydrogen desorption capacity. As shown in Figure 3c, a stable hydrogen uptake and release process could be achieved for $NaAlH_4$-$TiO_2$@C successfully under only light irradiation with a reversible capacity of 4 wt% after 10 cycles, corresponding to a capacity retention of 85%. XRD patterns (Figure 3e) demonstrate that $NaAlH_4$ is still the dominant phase in $NaAlH_4$-$TiO_2$@C after 10 cycles of hydrogenation process with only slight amount of $Na_3AlH_6$ and Al detected, which provides additional evidence to the excellent cycling stability of $NaAlH_4$-$TiO_2$@C under light irradiation. Correspondingly, the UV–vis–NIR spectrum of $NaAlH_4$-$TiO_2$@C after cycling remained basically the same as the as-milled sample (Figure 3f), indicating a stable light absorbance and photothermal effect of the material during cycling. The well-preserved photothermal performance upon cycling contributes to stable light-driven reversibility of $NaAlH_4$.

### 2.4. Universality of Light-Driven Hydrogen Storage

The reversible hydrogen uptake and release performance of $NaAlH_4$-$TiO_2$@C with light as the only energy source validates the idea of light-driven reversible hydrogen storage via coupling photothermal and catalytic effects. To take one step further, we would like to emphasize that this strategy is applicable to other metal hydrides, e.g., $LiAlH_4$ and $MgH_2$, that are known with moderate hydrogen desorption temperatures upon catalysis.[13] Since $TiO_2$ has been demonstrated previously as an effective catalyst for hydrogen desorption from $LiAlH_4$ and $MgH_2$,[14] the as-synthesized $TiO_2$@C in this study is directly adopted to evaluate the light-driven hydrogen storage performance of both $LiAlH_4$ and $MgH_2$. Indeed, upon introducing $TiO_2$@C, the temperature required for complete dehydrogenation of $LiAlH_4$ and $MgH_2$ could be effectively reduced to 175 and 290 °C from 210 and 380 °C, respectively (Figure S10, Supporting Information); meanwhile, the light absorbance of $LiAlH_4$ and $MgH_2$ could be effectively enhanced by $TiO_2$@C (**Figure 4**a,d). According to the relationship between material temperature

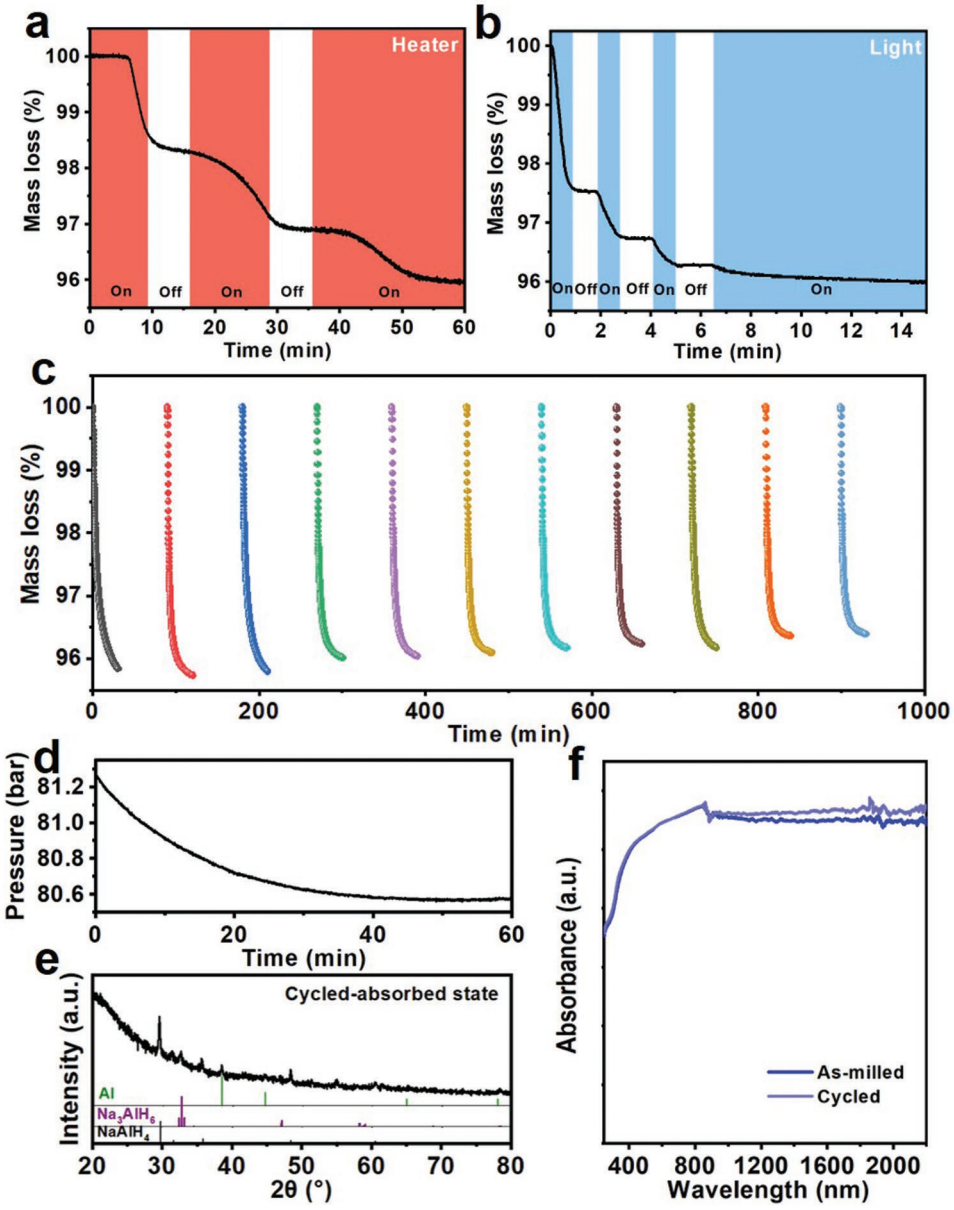


**Figure 3.** Response test of the hydrogen release process of $NaAlH_4$-$TiO_2$@C to a) electric heater and b) light. c) Hydrogen release profiles during the light-driven cycling test of $NaAlH_4$-$TiO_2$@C. d) Pressure change during light-driven hydrogenation process. e) XRD pattern of cycled $NaAlH_4$-$TiO_2$@C in absorbed state. f) UV–vis–NIR spectra of as-milled and cycled $NaAlH_4$-$TiO_2$@C in absorbed state.

and light intensity as evidenced above, the light intensity applied for $LiAlH_4$-$TiO_2$@C and $MgH_2$-$TiO_2$@C is determined to be 10 and 22 sun, respectively, to fulfill the requirements of their hydrogen desorption temperatures. The equilibrium temperature of $LiAlH_4$-$TiO_2$@C under 10 sun reaches 195 °C, enabling a rapid dehydrogenation within a time period of only 10 min (Figure 4b). The formation of LiH and Al, accompanied by the disappearance of $LiAlH_4$, provides additional evidence on complete dehydrogenation of $LiAlH_4$ (Figure 4c).

In terms of $MgH_2$-$TiO_2$@C, the equilibrium temperature is detected to be ≈270 °C under a light intensity of 22 sun and this value is lowered to 240 °C during hydrogenation under a hydrogen pressure of 5 bar, which is caused by the fact that the high thermal conductivity of hydrogen atmosphere[15] accelerates heat dissipation to the environment. Impressively, a reversible capacity of 3.7 wt% could be obtained for $MgH_2$-$TiO_2$@C under light irradiation and the slight degradation of reversible capacity could be attributed to the reaction between $MgH_2$ and $TiO_2$@C during the cycling process, leading to the consumption of active Mg with the formation of MgO as revealed by the XRD pattern (Figure 4f). Nevertheless, XRD pattern confirms the formation of Mg and the disappearance of $MgH_2$ after $H_2$ desorption under a light intensity of 22 sun, which directly confirms the complete dehydrogenation of $MgH_2$. Therefore, these results demonstrate the universality of light-mediated catalytic strategy to realize reversible hydrogen

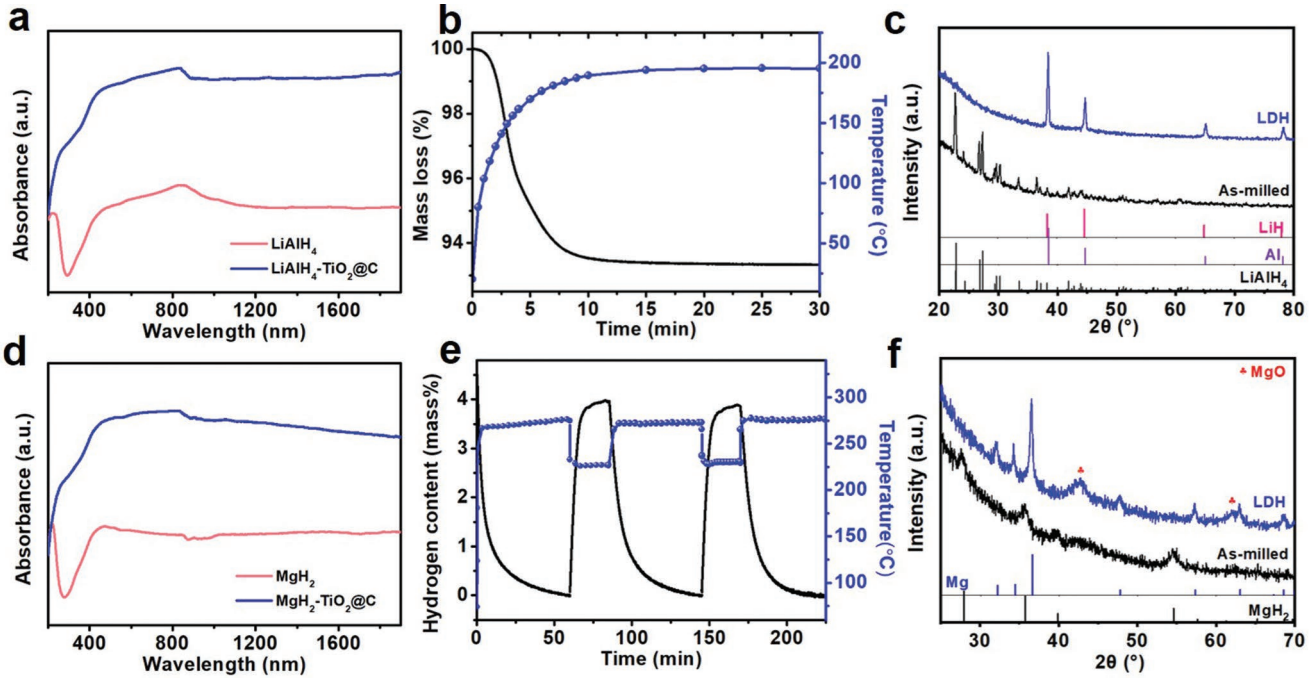


**Figure 4.** a) UV–vis–NIR spectra of $LiAlH_4$ and $LiAlH_4$-$TiO_2$@C. b) Temperature and hydrogen release profile of $LiAlH_4$-$TiO_2$@C under a light intensity of 10 sun. c) XRD patterns of $LiAlH_4$-$TiO_2$@C before and after light-driven hydrogen release. d) UV–vis–NIR spectra of $MgH_2$ and $MgH_2$-$TiO_2$@C. e) Temperature and hydrogen release/uptake profiles of $MgH_2$-$TiO_2$@C during the light-driven cycling test under a light intensity of 22 sun. f) XRD patterns of $MgH_2$-$TiO_2$@C before and after light-driven cycling.

storage in metal hydrides via matching the photothermal temperature of the material with the temperature required for its hydrogen storage reactions.

## 3. Conclusions

Reversible hydrogen storage in light-weight metal hydrides is realized using light as the only energy input based on a proposed light-mediated catalytic strategy via coupling photothermal effect and catalytic effect. Taking $NaAlH_4$ as a model example, $TiO_2$@C is constructed to integrate the catalytic effect of $TiO_2$ for lowering the operating temperature of $NaAlH_4$ down to 170 °C, and the photothermal effect of C for increasing the temperature of $NaAlH_4$ to 220 °C under light irradiation. As a result, when using $TiO_2$@C as the photothermal catalyst, light-driven complete hydrogen desorption from $NaAlH_4$ is achieved within 7 min under 10 sun light irradiation. More importantly, owing to the stable photothermal and catalytic effect of $TiO_2$@C, an excellent light-driven hydrogen storage reversibility of $NaAlH_4$ is realized, with a capacity of 4 wt% after 10 cycles, validating the concept of light-driven reversible hydrogen storage in metal hydrides. In addition, the proposed strategy is verified to be universal and applicable to other metal hydrides, e.g., $LiAlH_4$ and $MgH_2$. Despite the relatively high light intensity applied in this study, the concept and strategy established herein provides an alternative approach to electric heating. With improved composition- and structure- engineering of materials, accompanied by system design to limit heat dissipation, the light intensity required for light-driven hydrogen storage can be potentially lowered, allowing the design of reversible high-density hydrogen storage systems that do not rely on artificial energy.

## Supporting Information

Supporting Information is available from the Wiley Online Library or from the author.

## Acknowledgements

This work was financially supported by the National Key R&D Program of China (No. 2020YFA0406204), National Natural Science Foundation of China (22109026, 51971065, 51901045, U2130208), National Science Fund for Distinguished Young Scholars (51625102), the Science and Technology Commission of Shanghai Municipality (No. 21ZR1407500), and the Innovation Program of Shanghai Municipal Education Commission (2019-01-07-00-07-E00028).

## Conflict of Interest

The authors declare no conflict of interest.

## Data Availability Statement

The data that support the findings of this study are available in the supplementary material of this article.

## Keywords

catalysis, hydrogen storage, metal hydrides, photothermal effect, sodium alanate

Received: May 13, 2022
Revised: July 12, 2022
Published online:

[1] A. Schneemann, J. L. White, S. Kang, S. Jeong, L. F. Wan, E. S. Cho, T. W. Heo, D. Prendergast, J. J. Urban, B. C. Wood, M. D. Allendorf, V. Stavila, *Chem. Rev.* **2018**, *118*, 10775.

[2] Y. Huang, G. Xia, J. Zhang, Z. Guo, X. Yu, *Energy Storage Mater.* **2019**, *17*, 178.

[3] a) N. A. Ali, M. Ismail, *Int. J. Hydrogen Energy* **2021**, *46*, 766; b) Z. Ren, X. Zhang, Z. Huang, J. Hu, Y. Li, S. Zheng, M. Gao, H. Pan, Y. Liu, *Chem. Eng. J.* **2022**, *427*, 131546.

[4] a) W. Chen, L. You, G. Xia, X. Yu, *J. Mater. Sci. Technol.* **2021**, *79*, 205; b) U. Jeong, H. Kim, S. Ramesh, N. A. Dogan, S. Wongwilawan, S. Kang, J. Park, E. S. Cho, C. T. Yavuz, *Angew. Chem.* **2021**, *133*, 22652.

[5] E. Ianni, M. V. Sofianos, M. R. Rowles, D. A. Sheppard, T. D. Humphries, C. E. Buckley, *Int. J. Hydrogen Energy* **2018**, *43*, 17309.

[6] a) K. Xian, M. Wu, M. Gao, S. Wang, Z. Li, P. Gao, Z. Yao, Y. Liu, W. Sun, H. Pan, *Small* **2022**, https://doi.org/10.1002/smll.202107013; b) W. Zhu, L. Ren, C. Lu, H. Xu, F. Sun, Z. Ma, J. Zou, *ACS Nano* **2021**, *15*, 18494.

[7] a) D. Mateo, J. L. Cerrillo, S. Durini, J. Gascon, *Chem. Soc. Rev.* **2021**, *50*, 2173; b) L. Wang, Y. Dong, T. Yan, Z. Hu, A. A. Jelle, D. M. Meira, P. N. Duchesne, J. Y. Y. Loh, C. Qiu, E. E. Storey, Y. Xu, W. Sun, M. Ghoussoub, N. P. Kherani, A. S. Helmy, G. A. Ozin, *Nat. Commun.* **2020**, *11*, 2432.

[8] a) D. Rafi ud, Q. Xuanhui, L. Ping, L. Zhang, W. Qi, M. Z. Iqbal, M. Y. Rafique, M. H. Farooq, D. Islam ud, *J. Phys. Chem. C* **2012**, *116*, 11924; b) G.-J. Lee, J.-H. Shim, Y. W. Cho, K. S. Lee, *Int. J. Hydrogen Energy* **2008**, *33*, 3748.

[9] a) B. Han, Y.-L. Zhang, Q.-D. Chen, H.-B. Sun, *Adv. Funct. Mater.* **2018**, *28*, 1802235; b) H.-C. Yang, Z. Chen, Y. Xie, J. Wang, J. W. Elam, W. Li, S. B. Darling, *Adv. Mater. Interfaces* **2019**, *6*, 1801252.

[10] a) X. Zhang, Y. Liu, K. Wang, M. Gao, H. Pan, *Nano Res.* **2015**, *8*, 533; b) Y. Liu, X. Zhang, K. Wang, Y. Yang, M. Gao, H. Pan, *J. Mater. Chem. A* **2016**, *4*, 1087.

[11] a) J. Tian, X. Hu, H. Yang, Y. Zhou, H. Cui, H. Liu, *Appl. Surf. Sci.* **2016**, *360*, 738; b) S. Chen, Y. Xiao, Y. Wang, Z. Hu, H. Zhao, W. Xie, *Nanomaterials* **2018**, *8*, 245.

[12] X. Kang, Z. Fang, L. Kong, H. Cheng, X. Yao, G. Lu, P. Wang, *Adv. Mater.* **2008**, *20*, 2756.

[13] a) K. Wang, X. Zhang, Y. Liu, Z. Ren, X. Zhang, J. Hu, M. Gao, H. Pan, *Chem. Eng. J.* **2021**, *406*, 126831; b) L. Dan, H. Wang, J. Liu, L. Ouyang, M. Zhu, *ACS Appl. Energy Mater.* **2022**, *5*, 4976; c) X. L. Zhang, Y. F. Liu, X. Zhang, J. J. Hu, M. X. Gao, H. G. Pan, *Mater. Today Nano* **2020**, *9*, 100064; d) N. Sazelee, M. Ismail, *Int. J. Hydrogen Energy* **2021**, *46*, 9123.

[14] a) M. Ismail, Y. Zhao, X. B. Yu, I. P. Nevirkovets, S. X. Dou, *Int. J. Hydrogen Energy* **2011**, *36*, 8327; b) M. Zhang, X. Xiao, X. Wang, M. Chen, Y. Lu, M. Liu, L. Chen, *Nanoscale* **2019**, *11*, 7465; c) M. Zhang, X. Xiao, B. Luo, M. Liu, M. Chen, L. Chen, *J. Energy Chem.* **2020**, *46*, 191.

[15] M. L. Huber, A. H. Harvey, in *CRC Handbook of Chemistry and Physics*, CRC Press, Boca Raton, FL **2011**.